Supporting Information for

UNDERSTANDING CHEMICAL VS. ELECTROSTATIC SHIFTS IN X-RAY PHOTOELECTRON SPECTRA OF ORGANIC SELF-ASSEMBLED MONOLAYERS

Thomas C. Taucher,[1§] Iris Hehn,[1§] Oliver T. Hofmann,[1] Michael Zharnikov,[2] and Egbert Zojer[1]*

[1] Institute of Solid State Physics, NAWI Graz, Graz University of Technology, Petersgasse 16, A-8010 Graz, Austria.

[2] Angewandte Physikalische Chemie, Universität Heidelberg, Im Neuenheimer Feld 253, 69120 Heidelberg, Germany

§ T.C.T. and I.H. contributed equally.

* corresponding author: egbert.zojer@tugraz.at

S1. Simulation details of the pre-optimization using molecular dynamics

The potential energy surface (PES) of the C10EC5 alkyl thiolate SAM is rather complex including many local minima. To efficiently sample this PES we combined the DFT-based geometry optimization as described in the main manuscript with a pre-optimization using molecular dynamics (MD). To run the simulations the program package LAMMPS (v. 14 Feb 2013)[1] was applied. The Verlet[2] algorithm was used to solve the equations of motion in time steps of 1fs. The SHAKE[3] algorithm was employed for constraining the mobility of the hydrogen atoms during the simulation. For temperature slopes we chose an NVE ensemble (Berendsen thermostat)[4] and in the equilibration phase an NVT ensemble with the Nosé-Hoover[5,6] thermostat was used. Coulomb interactions were calculated in reciprocal space with the particle-particle-particle-mesh (PPPM)[7] method. The atomic charges needed were calculated for an isolated molecule using the ESP charge-partitioning scheme[8,9], where the charges are assigned to reproduce the quantum-mechanically calculated electrostatic potential at points selected according to the Merz-Singh-Kollman scheme.[8,9] Gaussian09[10] with the B3LYP[11–14] functional and an aug-cc-pVTZ[15–18] basis set were used for this calculation.

For most interactions the CHARMM36 general force field[19] (v. 2b7) was used. However, the gold-organic interactions were described with the GoIp[20] force field, which we found to be most appropriate for modelling organic adsorbates, and the Au-S bond was described with the potential designed by Jang et al.[21] This potential is of a modified Buckingham type and allows bond breaking, thus allowing the molecules to move on the substrate. Hence, we do not predetermine the bonding sites already with the starting configuration. The cutoff radius for pairwise interactions was chosen as 12 Å for Au-S. The Lenard-Jones potential

(lj/charmm/coul/long) used for the CHARMM force field had an inner cutoff radius of 12 Å and an outer one of 14 Å.

The Au(111) surface in the MD run was represented by ten layers of gold. The positions of the gold atoms were kept fixed during the simulation. Periodic boundary conditions in x- and y-direction were employed, creating a 2D infinite slab. The lateral extension of the periodic unit cell was chosen such that it contained 16 C10EC5 molecules in dense packing. At the start, all molecules were oriented upright with the same twist angle (i.e., not introducing any bias towards a herringbone arrangement of the molecules). To reach the global minimum we employed a temperature ramp, first heating the sample to T = 750 K (over a timespan of t = 0.2 ns). This allows the molecules to move freely on the substrate and lifts any bias incurred by the arbitrarily chosen starting configuration. The sample was then cooled to room temperature (T = 300 K) over t = 1.3 ns with a constant cooling rate and equilibrated there for t = 5 ns. Afterwards the system was slowly cooled to T = 0 K over a timespan of t = 4 ns to prevent thermal motion of the molecules, thus giving us straight molecular geometries without thermally induced “defects” in the final geometry. From the final structure, four representative molecules were picked and a unit cell containing five layers of gold substrate and four molecules was created for further geometry optimization using density functional theory (DFT).

S2. Details of the PAW potentials used for VASP calculations

Table S1 lists the PAW potentials used for all VASP calculations in this work, except the “VASP soft PAW” test calculation shown in Figure S1. For this test calculation soft PAW potentials were used for carbon and oxygen atoms.

Table S1. List of PAW potentials used for VASP calculations in this work.

Au	PAW_PBE Au 06Sep2000
S	PAW_PBE S 17Jan2003
C	PAW_PBE C 08Apr2002
H	PAW_PBE H 15Jun2001
O	PAW_PBE O 08Apr2002
F	PAW_PBE F 08Apr2002

S3. Testing different PAW potentials and comparison to a full potential code

In Figure S1 we compare C 1s energies of the C10EC5 SAM calculated with different PAW potentials to estimate the influence of the set of used potentials. As a reference we use results obtained with the full potential code FHI-aims[22] for the same system.

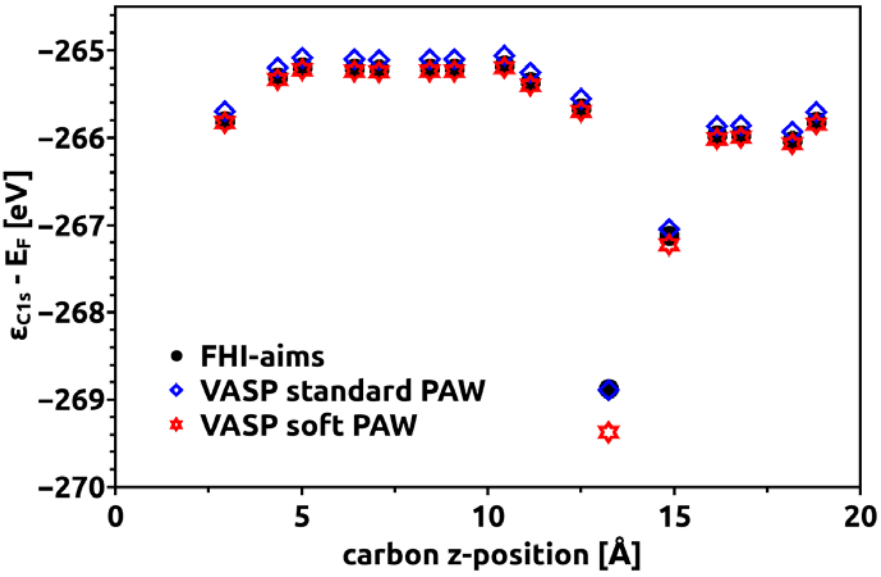

Figure S1. *C 1s energies of the full coverage C10EC5 SAM calculated with VASP using standard PAW potentials (Au, S, C, H, O) (open blue diamonds) and partially soft PAW potentials (Au, S, C_s, H, O_s) (open red stars). The results are compared to those obtained*

using the full potential code FHI-aims[22] *(full black dots) employing "tight" settings for all elements, except sulfur, for which "light" settings have been used. For the sake of comparing the different calculation methods all core-level energies shown in this plot are unscreened energies.*

The result of the VASP calculation using standard PAW potentials is nearly identical to the FHI-aims calculation, save for a small rigid offset. The calculation performed with soft PAW potentials for carbon and oxygen, however, differs noticeably from the other two calculations at the carbonyl carbon (the carbon lowest in energy and chemically most different).

S4. The impact of screening on calculated C 1s energies

Figure S2 shows a scatter plot of the carbon 1s core-level energies of a full coverage F8H11SH SAM. We compare the unscreened values with the ones including screening effects.

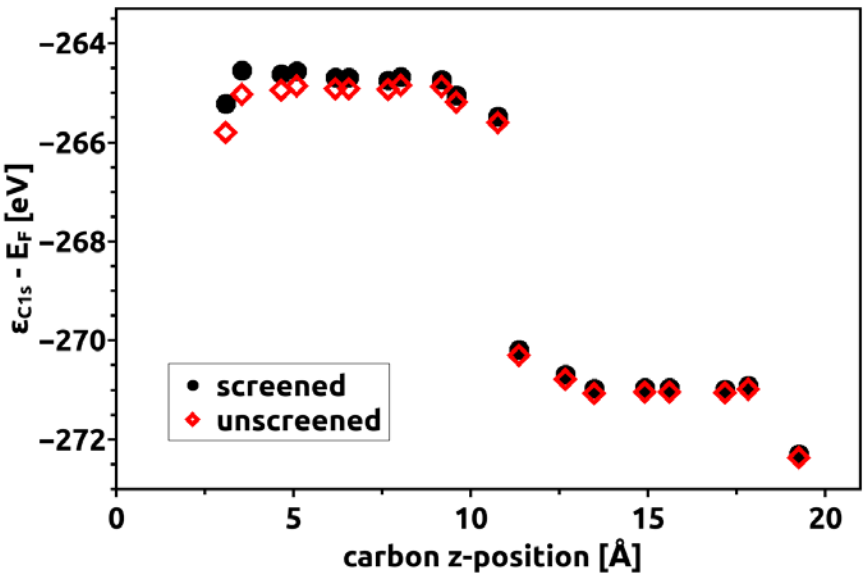

Figure S2. *Calculated C 1s core-level energies of a full coverage partially fluorinated alkyl thiolate SAM (F8H11SH) including (full black dots) and excluding (open red diamonds) screening effects by the metal.*

We see that the screening of the metal substrate shifts core-level energies to less negative values. Atoms closest to the substrate are affected the most, whereas there is practically no influence on atoms near the top of the SAM. Combined with the strong damping of the XPS signal of deep lying atoms (see next section) the impact of screening on the systems portrayed in this work is rather small.

S5. Impact of damping on calculated C 1s spectra

Figure S3 shows calculated XP spectra of the F8H11SH system including and excluding attenuation effects for the photoelectrons.

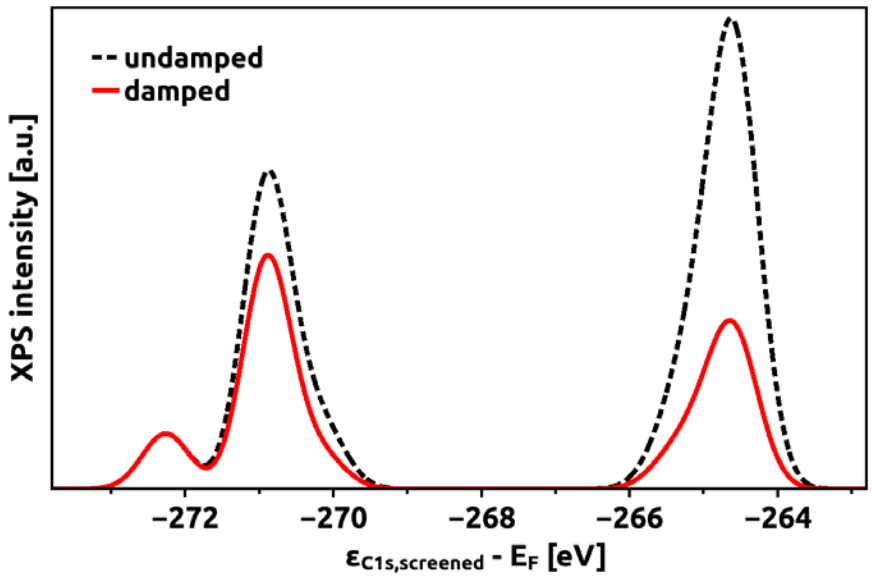

Figure S3. *Calculated XP spectra of a full coverage F8H11SH SAM, comparing a spectrum which takes an exponential attenuation of the signal into account (red solid line) and one neglecting it. Both curves include screening effects of the metal as described in the main article.*

We see that attenuation effects are significant. The intensity of the peak assigned to the bottom alkyl chain (at ≈ -265 eV) is reduced to about one third. The intensity of the fluorinated part of the molecule (≈ -271 eV) is only slightly reduced, as it constitutes the top part of the SAM. The CF_3 signal (≈ -272.5 eV) is unaffected by attenuation effects, because this carbon is situated right at the top of the SAM.

S6. Comparing non-stretched calculated XP spectra to experiments

Figures S4 and S5 compare the experimental XP spectra of full coverage F8H11SH and C10EC5 SAMs with calculated spectra which were only shifted and not stretched. They are included here for the sake of comparison to stress that the reproduction of the experimental trends/shifts by the simulations is by no means related to the commonly applied stretching of the energy scale of the Kohn-Sham eigenstates.

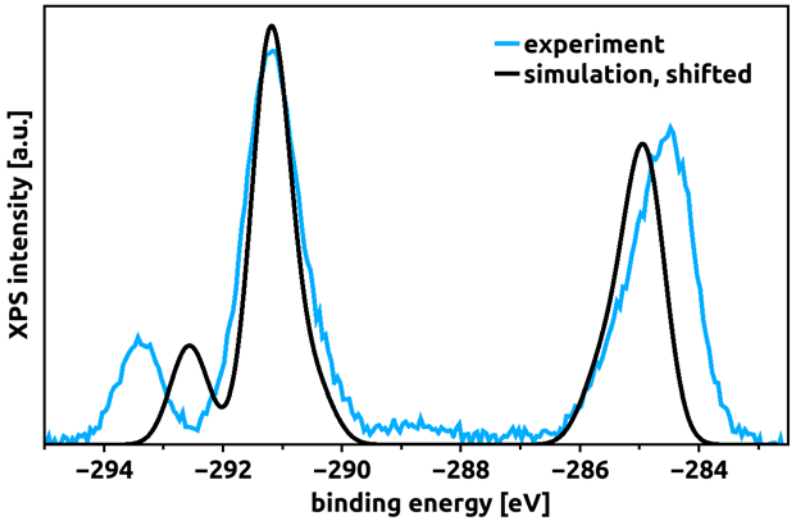

Figure S4. *Comparison of the measured HRXP spectrum*[23] *of a full coverage F8H11SH SAM on Au(111) (light blue) with the calculated spectrum (black). The calculated spectrum was rigidly shifted by -20.3eV to align the main peak with the experimental one, but not stretched. The*

measurements were performed with an incident photon energy of 580 eV. The experimental spectrum is reprinted with permission from (Lu, H.; Zeysing, D.; Kind, M.; Terfort, A.; Zharnikov, M. Structure of Self-Assembled Monolayers of Partially Fluorinated Alkanethiols with a Fluorocarbon Part of Variable Length on Gold Substrate. J. Phys. Chem. C 2013, 117, 18967–18979). Copyright (2013) American Chemical Society.

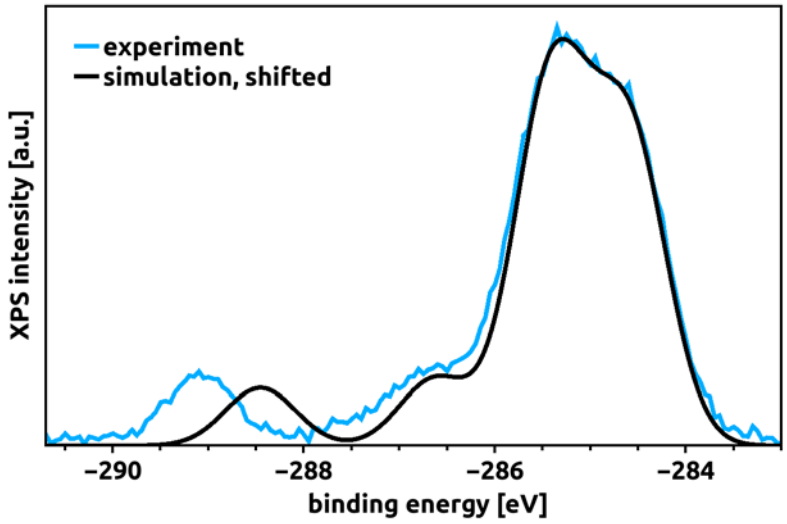

Figure S5. *Comparison of the measured HRXP spectrum*[24] *of a full coverage C10EC5 SAM on Au(111) (light blue) with the calculated spectrum (black). The calculated spectrum was rigidly shifted by -19.7eV to align the main peak with the experimental one, but not stretched. The measurements were performed with an incident photon energy of 580 eV. The experimental spectrum is reprinted with permission from (Cabarcos, O. M.; Shaporenko, A.; Weidner, T.; Uppili, S.; Dake, L. S.; Zharnikov, M.; Allara, D. L. Physical and Electronic Structure Effects of Embedded Dipoles in Self-Assembled Monolayers: Characterization of Mid-Chain Ester Functionalized Alkanethiols on Au{111}. J. Phys. Chem. C 2008, 112, 10842–10854). Copyright (2008) American Chemical Society.*

From Figures S4 and S5 we see that the calculated spectra, when only shifted rigidly without any stretching, qualitatively reproduce the measured ones quite accurately. All peaks found in the experimental spectra are present in the calculations and the relative peak intensities match. There are only slight differences regarding the exact values of the XPS peak shifts.

S7. Intermediate coverages

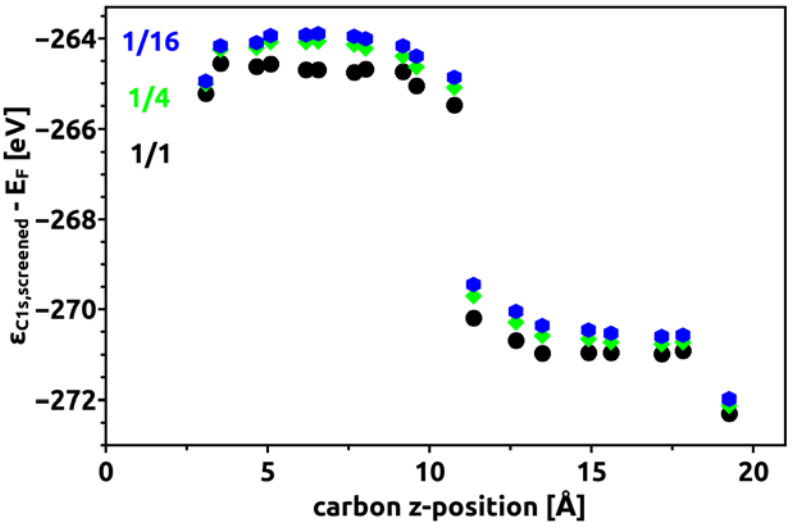

Figure S6. *Calculated C 1s core-level energies of F8H11SH SAMs at different coverages. We show three different coverages in this plot: full coverage (black dots), a coverage of 1/4 (green diamonds) and a coverage of 1/16 (blue hexagons). For the sake of comparison ε = 2.26 was used for calculating screening effects in all three cases shown here (in contrast to the main manuscript, where ε =1 was used at the lowest coverage).*

In Figure S6 we see that the results for full coverage and a coverage of 1/4 are still quite different from one another. However, coverages of 1/4 and 1/16 yield already pretty similar results. We

therefore interpret a coverage of 1/16 as dealing with isolated molecules on the substrate for the F8H11SH system. The case is a bit different for the C10EC5 SAM discussed next (see Figure S7), where it was necessary to reduce the coverage even more to eliminate collective electrostatic effects.

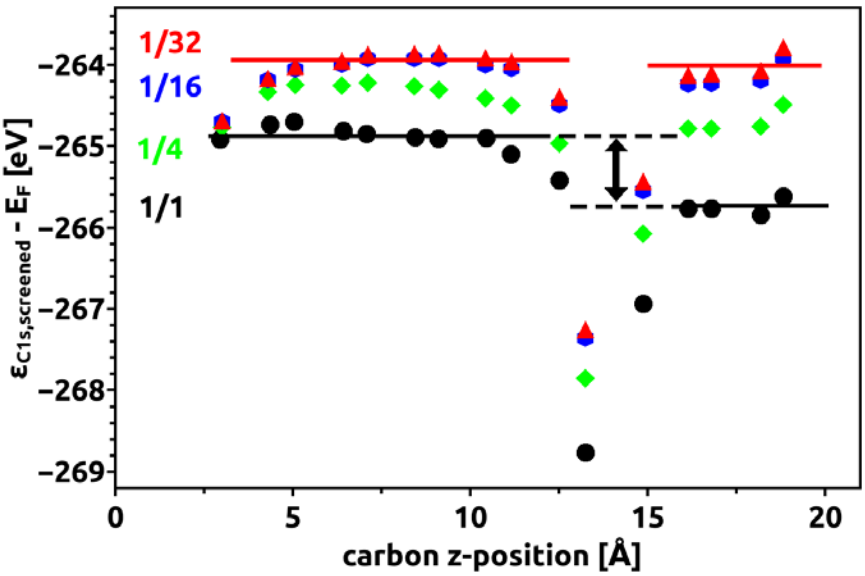

Figure S7. *Calculated C 1s core-level energies of C10EC5 SAMs with different coverages. The intermediate coverages that were calculated are included in this plot: full coverage (black dots), a coverage of 1/4 (green diamonds), a coverage of 1/16 (blue hexagons) and a coverage of 1/32 (red triangles). For the sake of comparison ε = 2.26 was used for calculating screening effects in all four cases shown here (in contrast to the main manuscript, where ε =1 was used at the lowest coverage).*

We see a trend going from full to low coverage, with the energetic difference between bottom and top segment gradually decreasing. The electrostatic shift of the bond dipole also vanishes

gradually from full to low coverage. The results for coverages 1/16 and 1/32 are already nearly identical. The electrostatic situation does not change anymore, the molecules behave as if isolated in both cases. For a coverage of 1/4 there still is some collective electrostatic interaction present, but much weaker than in the full coverage system. Thus, an electrostatic shift between bottom and top chain can still be seen, but it is much smaller than in the full coverage system.

References

(1) Plimpton, S. Fast Parallel Algorithms for Short-Range Molecular Dynamics. *J. Comput. Phys.* **1995**, *117*, 1–19.

(2) Verlet, L. Computer "Experiments" on Classical Fluids. I. Thermodynamical Properties of Lennard-Jones Molecules. *Phys. Rev.* **1967**, *159*, 98–103.

(3) Ryckaert, J.-P.; Ciccotti, G.; Berendsen, H. J. . Numerical Integration of the Cartesian Equations of Motion of a System with Constraints: Molecular Dynamics of N-Alkanes. *J. Comput. Phys.* **1977**, *23*, 327–341.

(4) Berendsen, H. J. C.; Postma, J. P. M.; van Gunsteren, W. F.; DiNola, A.; Haak, J. R. Molecular Dynamics with Coupling to an External Bath. *J. Chem. Phys.* **1984**, *81*, 3684.

(5) Nosé, S. A Unified Formulation of the Constant Temperature Molecular Dynamics Methods. *J. Chem. Phys.* **1984**, *81*, 511.

(6) Hoover, W. G. Canonical Dynamics: Equilibrium Phase-Space Distributions. *Phys. Rev. A* **1985**, *31*, 1695–1697.

(7) Hockney, R. W.; Eastwood, J. W. *Computer Simulation Using Particles*; McGraw-Hill International Book Co: New York, 1981.

(8) Singh, U. C.; Kollman, P. A. An Approach to Computing Electrostatic Charges for Molecules. *J. Comput. Chem.* **1984**, *5*, 129–145.

(9) Besler, B. H.; Merz, K. M.; Kollman, P. A. Atomic Charges Derived from Semiempirical Methods. *J. Comput. Chem.* **1990**, *11*, 431–439.

(10) Frisch, M. J.; Trucks, G. W.; Schlegel, H. B.; Scuseria, G. E.; Robb, M. A.; Cheeseman, J. R.; Scalmani, G.; Barone, V.; Mennucci, B.; Petersson, G. A.; et al. *Gaussian09, Revision A.01*.

(11) Becke, A. D. Density-Functional Thermochemistry. III. The Role of Exact Exchange. *J. Chem. Phys.* **1993**, *98*, 5648.

(12) Lee, C.; Yang, W.; Parr, R. G. Development of the Colle-Salvetti Correlation-Energy Formula into a Functional of the Electron Density. *Phys. Rev. B* **1988**, *37*, 785–789.

(13) Vosko, S. H.; Wilk, L.; Nusair, M. Accurate Spin-Dependent Electron Liquid Correlation Energies for Local Spin Density Calculations: A Critical Analysis. *Can. J. Phys.* **1980**, *58*, 1200–1211.

(14) Stephens, P. J.; Devlin, F. J.; Chabalowski, C. F.; Frisch, M. J. Ab Initio Calculation of Vibrational Absorption and Circular Dichroism Spectra Using Density Functional Force Fields. *J. Phys. Chem.* **1994**, *98*, 11623–11627.

(15) Dunning, T. H. Gaussian Basis Sets for Use in Correlated Molecular Calculations. I. The Atoms Boron through Neon and Hydrogen. *J. Chem. Phys.* **1989**, *90*, 1007.
(16) Kendall, R. A.; Dunning, T. H.; Harrison, R. J. Electron Affinities of the First-Row Atoms Revisited. Systematic Basis Sets and Wave Functions. *J. Chem. Phys.* **1992**, *96*, 6796.
(17) Davidson, E. R. Comment on "Comment on Dunning's Correlation-Consistent Basis Sets." *Chem. Phys. Lett.* **1996**, *260*, 514–518.
(18) Woon, D. E.; Dunning, T. H. Gaussian Basis Sets for Use in Correlated Molecular Calculations. III. The Atoms Aluminum through Argon. *J. Chem. Phys.* **1993**, *98*, 1358.
(19) Vanommeslaeghe, K.; Hatcher, E.; Acharya, C.; Kundu, S.; Zhong, S.; Shim, J.; Darian, E.; Guvench, O.; Lopes, P.; Vorobyov, I.; et al. CHARMM General Force Field: A Force Field for Drug-like Molecules Compatible with the CHARMM All-Atom Additive Biological Force Fields. *J. Comput. Chem.* **2009**, 671–690.
(20) Iori, F.; Di Felice, R.; Molinari, E.; Corni, S. GolP: An Atomistic Force-Field to Describe the Interaction of Proteins with Au(111) Surfaces in Water. *J. Comput. Chem.* **2009**, *30*, 1465–1476.
(21) Jang, S. S.; Jang, Y. H.; Kim, Y.-H.; Goddard, W. A.; Flood, A. H.; Laursen, B. W.; Tseng, H.-R.; Stoddart, J. F.; Jeppesen, J. O.; Choi, J. W.; et al. Structures and Properties of Self-Assembled Monolayers of Bistable [2]Rotaxanes on Au (111) Surfaces from Molecular Dynamics Simulations Validated with Experiment. *J. Am. Chem. Soc.* **2005**, *127*, 1563–1575.
(22) Blum, V.; Gehrke, R.; Hanke, F.; Havu, P.; Havu, V.; Ren, X.; Reuter, K.; Scheffler, M. Ab Initio Molecular Simulations with Numeric Atom-Centered Orbitals. *Comput. Phys. Commun.* **2009**, *180*, 2175–2196.
(23) Lu, H.; Zeysing, D.; Kind, M.; Terfort, A.; Zharnikov, M. Structure of Self-Assembled Monolayers of Partially Fluorinated Alkanethiols with a Fluorocarbon Part of Variable Length on Gold Substrate. *J. Phys. Chem. C* **2013**, *117*, 18967–18979.
(24) Cabarcos, O. M.; Shaporenko, A.; Weidner, T.; Uppili, S.; Dake, L. S.; Zharnikov, M.; Allara, D. L. Physical and Electronic Structure Effects of Embedded Dipoles in Self-Assembled Monolayers: Characterization of Mid-Chain Ester Functionalized Alkanethiols on Au{111}. *J. Phys. Chem. C* **2008**, *112*, 10842–10854.